CRACKING DUE TO RESTRAINT STRESSES IN EARLY-AGE RADIATION SHIELDING WALL

Agnieszka KNOPPIK-WRÓBEL *

[a] MSc Eng.; Department of Structural Engineering, Silesian University of Technology, 44-100 Gliwice, Poland
E-mail address: *agnieszka.knoppik-wrobel@polsl.pl*

Abstract

Cracking in early-age concrete walls develops mainly due to thermal restraint stresses. These cracks are of great concern in the structures where strict tightness requirements are defined such as the walls of radiation shielding containments. The paper aims at defining major phenomena responsible for early-age cracking and discusses the main factors which influence these phenomena. Structural behaviour of early-age walls is presented on the example of a radiation shielding wall in which severe early-age cracking was observed. The currently used methods for structural analysis of early-age walls are referred to and discussed. It is shown that the analysis of such structures can be performed with simple approaches suitable for manual calculations if the behaviour of the analysed structure is understood. The cracking risk in walls depends mostly on the temperature change during cooling, thermal gradient at the thickness of the wall and the degree of restraint. The degree of restraint should be limited by construction of the wall in short segments; as the degree of restraint is a known value, the design, execution and curing of the wall should concentrate on limitation of the temperature change to a calculated value. In the important structures the temperature development should be continuously measured and its unexpected changes should be instantaneously accommodated.

Streszczenie

Wczesne rysy termiczno-skurczowe w ścianach betonowych powstają głównie w efekcie termicznych naprężeń wymuszonych. Rysy te są poważnym problemem w konstrukcjach, dla których określone są rygorystyczne wymagania szczelności, takich jak ściany obudów ochrony radiologicznej. Celem artykułu jest zdefiniowanie głównych zjawisk odpowiedzialnych za powstawanie tych rys oraz omówienie głównych czynników mających wpływ na te zjawiska. Zachowanie ścian wykonanych z młodego betonu zostało przedstawione na przykładzie obudowy ochrony radiologicznej, w której we wczesnym wieku zaobserwowano poważne rysy. Przywołano oraz omówiono obecnie stosowane metody analizy zachowania ścian betonowych we wczesnych fazach dojrzewania betony. Wykazano, zrozumienie zachowania tych konstrukcji pozwala na ich analiza przy użyciu prostych, manualnych metod obliczeniowych. Ryzyko zarysowania ścian zależy głównie od spadku temperatury podczas chłodzenia, gradientu temperatury na grubości ściany oraz stopnia skrępowania. Stopień skrępowania należy ograniczać poprzez realizację ściany w postaci krótkich segmentów; jako że stopień skrępowania jest wartością znaną, projektowanie, wykonawstwo oraz pielęgnacja ściany podczas jej dojrzewania powinny koncentrować się na ograniczeniu temperatury do wyznaczonej wartości. W odpowiedzialnych konstrukcjach temperatura powinna być mierzona w sposób ciągły, a jej niezamierzone zmiany powinny być natychmiastowo korygowane.

K e y w o r d s : **Early-age cracking; Radiation shielding; Reinforced concrete wall; Restraint stresses.**

1. INTRODUCTION

Reinforced concrete walls are subjected to high values of tensile stresses in early phases of concrete hardening which may lead to their cracking. The origin of these stresses are volume changes caused by variations of the elements' temperature and moisture content accompanying the process of cement hydration. There is a number of interrelated phenomena occurring simultaneously in concrete during its early ages. The most significant is the heat flow between the element and the environment. It is driven by temperature dif-

ference between the self-heated element and the (usually) cooler surrounding air. The volume changes caused by temperature variations are inherent of concrete and significant in any concrete structure whose dimensions predispose the heat to be produced at the rate greater than it dissipates. However, the effect of the volume changes on the stresses arising in a young concrete structure is determined mainly by the geometry, support and boundary conditions. Consequently, the resulting cracking pattern differs between different concrete structures.

In reinforced concrete walls stresses result from a coupled action of self-induced and restraint stresses. Self-induced stresses are induced by the internal restraint caused by temperature gradients and their influence depends mostly on the thickness of the element. Restraint stresses result from external limitation of deformation exerted by a restraining body (rock or previously cast layers of concrete), which most often has a character of a linear restraint along one or more edges of the element. Their magnitude depends on a degree of restraint induced by the restraining body. In reinforced concrete walls the restraint stresses play a predominant role [1].

The cracks which appear in early ages of reinforced concrete walls hardening have non-mechanical origin and occur even before the design load is applied. This does not mean, however, that these cracks are of no concern and that the problem of early-age cracking of walls is negligible. In contrary – due to restrained contraction of the wall numerous cracks can appear on the whole length of the wall, reaching considerable heights (even whole height of the wall), with widths by far exceeding allowable limits and some of the cracks being through cracks. This may handicap the structure before it is put into operation, let alone its durability during the designed utilisation period. Cracking of concrete is especially undesirable in structures with harsh tightness requirements, such as liquid tank walls or radiation shielding walls, in which cracks would promote leakage of toxic substances into the environment.

Early-age cracking in externally restrained structures is still very common. It may seem that the behaviour of early-age walls is well-understood: there have been multiple works published on this topic [2, 3] and problem was covered by several international standards [4, 5, 6]. However, due to overwhelming amount of proposals and recommendations it appears that there is still a need to provide a concise description of the mechanisms of major phenomena occurring in the structures in question.

Hence, the aim of this paper is to define major phenomena responsible for cracking of reinforced concrete walls during early phases of concrete hardening and main factors which influence these phenomena. The paper presents structural behaviour of early-age walls; as an example an X-ray radiation shielding wall is discussed. The proposals for description of its behaviour are referred to and their approach to description of the constitutive phenomena is compared and discussed. The paper aims to present a concise description of the origin of early-age cracking which will help to understand the causes of damage in existing structures as well as design and execute new robust structures.

2. EARLY-AGE STRESSES IN RC WALLS

2.1. Mechanism of generation of early-age stresses

Stresses developing in early-age reinforced concrete walls due to thermal and shrinkage volume changes are caused by both self-induced and restraint stresses. The character and values of the stresses in medium-thick concrete elements are governed mainly by the temperature variations [1]. When the structure is improperly cured, intensive drying on the surface of the wall may appear which would lead to moisture content gradients and increase of total stresses due to shrinkage-induced stresses. In properly cured structures when the element matures in wet conditions, drying shrinkage poses little problem and is usually neglected in the analyses. Nevertheless, the hydration process is connected with bounding of water by hydrating cement which leads to decrease in overall volume of the hardening element. The resulting shrinkage is referred to as autogenous shrinkage and it is uniform over the volume of the element.

Self-induced stresses are generated due to the gradients of temperature within the volume of the structure, in case of walls especially at the thickness of the wall. Their magnitude depends directly on the magnitude of the gradient and increases as the massiveness of the element increases [1]. The massiveness of the element, m, is a ratio between the total area of surfaces of heat exchange with the environment, S, and the total volume of the element, V, [4]:

$$m = \frac{S}{V}.$$
(1)

However, to evaluate the massiveness of an element regarding the temperature gradients, the equivalent thickness of the element, d_e, is advised to be used, which represents the shortest path through which the
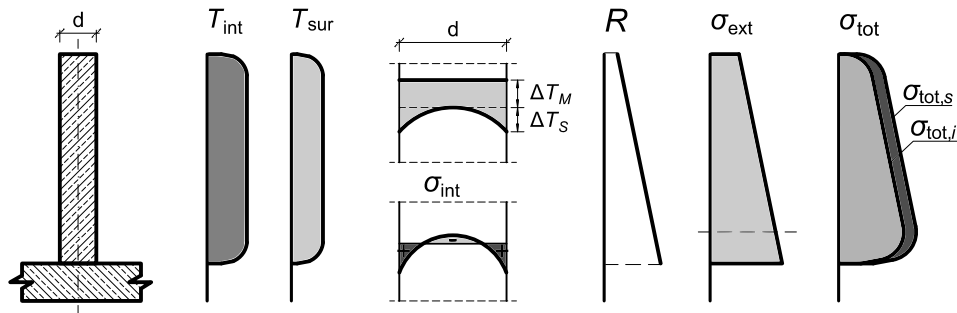
Figure 1.
Early-age thermal stresses in reinforced concrete wall

heat can be transported from the interior of the element to the surrounding environment [7]. For elements with simple geometry such as prismatic walls the equivalent thickness is a reciprocal of the massiveness m. The greater the equivalent thickness, the longer is the path and the higher are the foreseeable temperature gradients (for identical material properties and boundary conditions).

Restraint stresses are caused by external limitation of deformation. In case of reinforced concrete walls such a restraint exists along one or more edges of the wall and is exerted by the mature concrete of previous layers (foundation, previous segments of the wall). The magnitude of restraint stresses depends on a degree of restraint, expressed with the restraint factor, R, which in any point of the element is defined as a ratio between the stress generated in an unrestrained element, σ, to the fixation stress, σ_{fix}, [2, 4, 5]:

$$R = \frac{\sigma}{\sigma_{fix}}. \tag{2}$$

The degree of restraint of the element depends on the length-to-height ratio, L/H, and on the ratio of stiffness of the element and the restraining body.

Fig. 1 presents distribution of temperature, T, and total stresses, σ_{tot}, in a typical early-age wall. The wall is subjected to tensile stresses in the cooling phase which are caused by restrained elongation of the wall due to temperature change, ΔT_M. These tensile stresses are higher at the surface than in the interior of the wall. This is caused by the temperature gradients: temperature in the interior, T_{int}, is different than temperature at the surface, T_{sur}, so additional tensile stress of self-induced character is caused by temperature difference, ΔT_S. The stresses generated in the wall are induced by the bond forces which

develop at the construction joint between the adjacent concrete layers. The bond force subjects the wall to eccentric tension with respect to the neutral axis of the element. Distribution of tensile stress at the height of the section is proportional to the distribution of the restraint, $R(h)$ (restraint stress due to external restraint, σ_{ext}, is proportional to the degree of restraint), and depends on the temperature gradient at the height of the wall.

2.2. Calculation of early-age stresses

To account for the fact that the stresses in early-age walls result from a coupled action of internal and external restraints, a compensation plane method was introduced in Japanese standard for concrete design [5] for calculation of stresses occurring in early-age walls. The approach similar to compensation plane method was introduced in several standards worldwide [4, 6]. These standards but also other authors [2, 3] proposed the approaches to determine the values of the restraining coefficients and elaborated on the factors which influence the degree of restraint. The detailed comparison and discussion of these approaches was presented in [8].

According to that approach the increment of stress due to the internal restraint can be determined from the difference between the strain value at a point of the compensation line, ε_{comp}, and the thermal strain distribution curve, ε_0, (Fig. 2) by the equation:

$$\sigma_{int} = E_c \left(\varepsilon_0 - \varepsilon_{comp} \right). \tag{3}$$
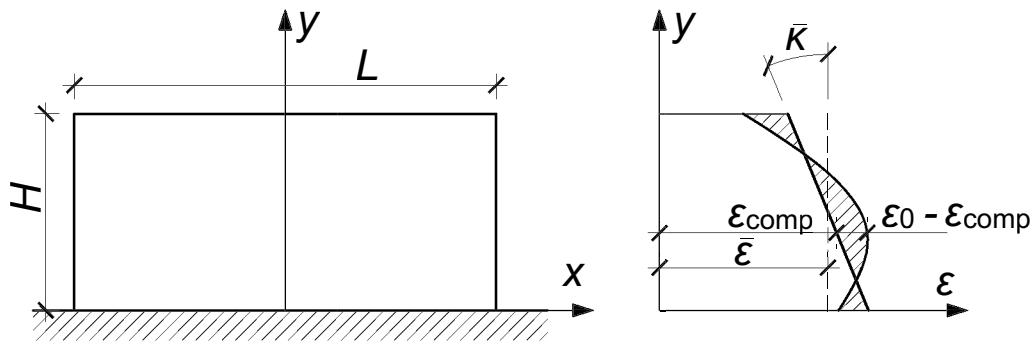
Figure 2.
Determination of self-induced stresses in wall according to CPM [5]

The external restraint acts against axial deformation and flexural deformation, as shown in Fig. 3. A free deformation of the concrete element can be separated into deformation in an axial direction (expansion or contraction, $\bar{\varepsilon}$) and flexural deformation in a vertical direction, $\bar{\kappa}$. The forces resulting from the restraint of these two deformations can be calculated as follows:

$$\begin{aligned} N_R &= R_N E_c A \bar{\varepsilon} \\ M_R &= R_M E_c I \bar{\kappa} \end{aligned} \qquad (4)$$

where:

R_N, R_M – translational and rotational restraint factor;

E_c – modulus of elasticity of concrete;

A, I – cross-section and modulus of inertia of the wall.
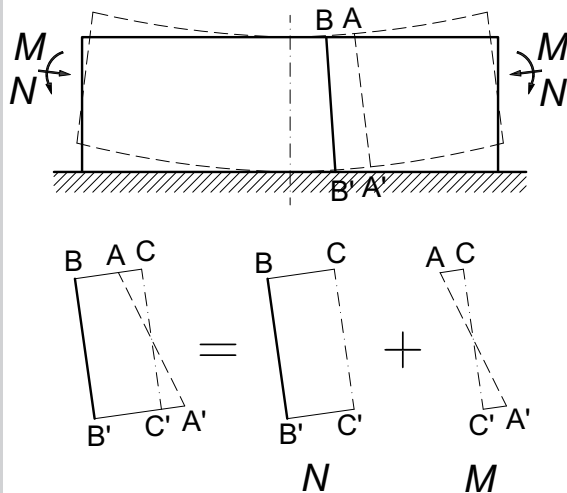
Figure 3.
Determination of restraint stresses in wall according to CPM [5]

The resulting restraint stress is caused by the coupled action of axial force and bending moment and can be calculated with the use of equation:

$$\sigma_{\text{ext}} = \frac{N_R}{A} + \frac{M_R}{I}(y - y_{\text{cen}}), \qquad (5)$$

where $(y - y_{\text{cen}})$ is a distance from the joint to the neutral axis of the wall.

The values of restraining coefficients vary from point to point in the element according to the degree of restraint. The degree of restraint depends on a number of factors, most of which result from the geometry of the wall. In the most general form the degree of restraint can be expressed with a restraint factor of a following form [2]:

$$R = R(R^0, \delta_{\text{res}}, \delta_{\text{slip}}). \qquad (6)$$

R^0 is a plane-section restraint factor which represents the translational and rotational restraint exerted by the restraining body. Determination of this restraint factor is simplified with the assumption that in most of the practical cases the walls are fully restrained against rotation and only translational restraint is calculated ($R^0 = R^0_N$), which depends on the stiffness of the restraining body. The translational restrain coefficient in such a form was proposed by Nilsson [2], in ACI Report 207 [4] and Eurocode 2 – Part 3 [6]. The plane-section restraint coefficient is a sufficient representation of the degree of restraint in the walls in which the plane-section hypothesis applies, so the walls which are characterised with a high length-to-height ratio. Nilsson [2] suggests that walls of $L/H > 5$ satisfy that condition. In the walls with lower value of L/H, so the walls in which the plane-section theory is no longer valid, the high-walls effects become more visible. The two predominant high-

walls effects are resilience and slip failure.

The resilience represents non-linear effects in high walls which are responsible for non-linear distribution of the degree of restraint at the height of the wall. The non-linear effects are more visible as the L/H decreases. Bluntly speaking, the resilience, expressed with a resilience factor, δ_{res}, would refer to the range of the height at which tensile stresses would develop in the restrained contracting wall. In the walls with higher value of L/H this range will be greater and so for extremely long walls, i.e. walls of $L/H > 10$, tensile stresses may cause cracking with cracks over the whole height of the wall. The resilience factor is a product of basic resilience factor and rotational and translational correction factors, but to simplify the resilience factor is taken as equal to the basic resilience factor $\delta_{res} = \delta_{res}^0$. Experimentally determined values for basic resilience factor were provided by ACI [4], JSCE [5] and Emborg [9].

Slip factor, δ_{slip}, is used to represent the effect of slip failure whose development in shorter walls may strongly influence the tensile stress distribution in central part of the wall and affect the cracking risk. The values of slip factor were numerically determined by Nilsson [2] for a wide range of geometries. Broken bond reduces the length at which the wall is restrained and as such modifies the distribution and values of the degree of restraint. Slip failure may occur as a result of coupled action of tensile force, which produces shear stresses at the joint, and bending moment, which produces stresses normal to the joint. When shear stresses at the joint exceed the bond strength slip occurs. To check if the slip failure is due to appear the value of the bond stress and bond strength must be calculated. The bonds stress can be calculated as [3]:

$$\tau(t) = \frac{A\,\bar{\varepsilon}\,E_c(t)}{0.25\,L\,B}, \tag{7}$$

where:

L, B – length and thickness of the wall;
A – cross-section area of the wall.

The bond strength is recommended by Flaga [3] to be calculated with Mörsch formula:

$$\bar{\tau}(t) = 0.5\sqrt{f_c(t)\,f_{ct}(t)}.$$

Acc. to Eurocode 2 [10] the bond strength between two concretes can be calculated as:

$$\bar{\tau}(t) = c\,f_{ctd}(t) + \mu\,\sigma_n + \rho\,f_{yd}(\mu\sin\alpha + \cos\alpha) \le 0.5\nu\,f_{cd}, \tag{8}$$

where:

c, μ – factors depending on the roughness of the interface;
f_{ctd} – design tensile strength of the concrete;
σ_n – stress per unit area caused by the minimum external normal force across the interface that can act simultaneously with the shear force, such as $\sigma_n < 0.6\,f_{cd}$. When σ_n is tensile, which happens during contraction od wall, ($c\,f_{ctd}$) should be taken as 0;
ρ – degree of reinforcement in the joint (area of reinforcement crossing the interface related to the area of the joint);
α – angle dependent on the indentation of the construction joint;
ν – effectivity factor.

The stress normal to the joint, σ_n, is induced as the wall is being rotated by the bending moment (see Fig. 3). The occurring stress may cause delamination of the wall and restraining body at the ends of the wall. The value of this normal stress can be determined with the use of vertical restraint factor. For walls with different restraining conditions the values of vertical restraint factors were given by Eurocode 3 – Part 3 [6].

The total strain which may lead to early-age cracking is caused by strain due to temperature change during cooling, ΔT, and shrinkage strain, ε_{sh}. Thermal strain is proportional to the temperature change according to the thermal dilation coefficient, α_T:

$$\varepsilon_T = \alpha_T\,\Delta T.$$

In analytic calculations it is convenient to assume a mean value of temperature at the thickness of the wall – the self-induced stresses are then neglected. The expected temperature increase related to the element's massiveness was proposed by Flaga [11]:

- in massive elements, $m < 2/m$: $\Delta T = 20 \div 50°C$;
- in medium-thick elements, $2/m \le m \le 15/m$: $\Delta T = 3 \div 20°C$;
- in thin elements, $m > 15/m$: $\Delta T = 1 \div 3°C$.

Since the cracking risk is predominantly dependent on the restraint stresses such an approach is justified. Determination of the exact thermal gradient would require solution of the heat equation:

$$c_b\,\rho\,\frac{\partial T}{\partial t} = \lambda\,\nabla^2 T + s, \tag{9}$$

where:

c_b, λ, ρ – specific heat [kJ/(kg K)], thermal conductivity [kJ/(s m K)] and density [kg/m³] of concrete;

s – source function which represents the rate of hydration heat development [kJ/(kg s)].

Solution to this second-order PDE can be found only with a numerical approach. For that purpose the Schmidt Method is advised. It is a simple finite difference method in which the temperatures are calculated in discrete nodes at discrete time steps. In each time step first the temperature distribution is calculated in the nodes by averaging the adjacent temperatures and then the adiabatic temperature rise over that time step is added. To solve the heat equation with Schmidt Method the simplest, first type boundary condition is applied which assumes that the temperature at the boundary, i.e. at the contact surface of the wall is equal to the ambient temperature. It is clearly visible, however, that the use of this method for manual calculations would be tedious and time-consuming.

Shrinkage strain is a sum of drying shrinkage strain, ε_{cd}, and autogenous shrinkage strain, ε_{ca}. According to Eurocode 2 [10] drying shrinkage strain can be calculated as follows:

$$\varepsilon_{cd}(t) = \beta_{ds}(t, t_0) k_h \, \varepsilon_{cd,0}, \tag{10}$$

where:

k_h – coefficient dependent on notional size of concrete element h_0 relating cross-section element to the perimeter in contact with atmosphere;

$\varepsilon_{cd,0}$ – free drying shrinkage strain;

$\beta_{ds}(t, t_0)$ – relationship defining the actual drying shrinkage at the moment, t, for a given moment of the beginning of drying process, t_s, given by the formula:

$$\beta_{ds}(t, t_0) = \frac{t - t_0}{(t - t_0) + 0.04\sqrt{h_0^3}}. \tag{11}$$

Development of autogenous shrinkage, which is crucial in early ages of concrete curing, can be defined by the function:

$$\varepsilon_{ca}(t) = \beta_{as}(t) \, \varepsilon_{ca,\infty}, \tag{12}$$

where:

$\varepsilon_{ca,\infty}$ – final value of autogenous shrinkage strain, defined for a given class of concrete acc. to its 28-day characteristic compressive strength f_{ck} [MPa] as:

$$\varepsilon_{ca,\infty} = 2.5(f_{ck} - 10) \cdot 10^{-6}, \tag{13}$$

$\beta_{as}(t)$ – relationship defining the actual autogenous shrinkage at time t:

$$\beta_{as}(t) = 1 - e^{(-0.2\sqrt{t})}. \tag{14}$$

Shrinkage strain can be expressed with substitute temperature change:

$$\Delta T_{sh} = \frac{\varepsilon_{sh}}{\alpha_T}. \tag{15}$$

It must be noted that the strain should be taken as differential strain (difference between strain in restraining body and restrained wall), not the total strain. It was recommended by Flaga [3] to determine differential thermal and shrinkage strain as follows:

$$\varepsilon_T^* = 0.9\varepsilon_T, \tag{16}$$

$$\varepsilon_{sh}^* = \varepsilon_{sh}^{II}(t^{II}) - \left[\varepsilon_{sh}^{I}(t^{I} + t^{II}) - \varepsilon_{sh}^{I}(t^{I})\right], \tag{17}$$

where:

$\varepsilon_{sh}^{II}(t^{II})$ – shrinkage strain of the wall at the moment of analysis (age of wall = t^{II}, days);

$\varepsilon_{sh}^{I}(t^{I} + t^{II})$ – shrinkage strain of the restraining body at the moment of analysis (age of restraining body = $t^{I} + t^{II}$, days);

$\varepsilon_{sh}^{I}(t^{I})$ – shrinkage strain of the restraining body at the moment of execution of the wall (age of restraining body = t^{I}, days).

Finally, there is a need to assume appropriate material model for early-age concrete which would account for ageing and viscous effects. A simple viscoelastic model is recommended for analytic calculations. The ageing is expressed with time-development of the material properties. There are two general approaches worldwide to define the time-development of the material properties: with exponential decaying function or with linear hyperbolic function. The exponential function as given by Model Code 2010 [12] and Eurocode 2 [10] has a form:

$$\beta_c(t) = e^{s\left[1 - \sqrt{28/t}\right]}, \tag{18}$$

The hyperbolic function as given by ACI Report 209 [13] and JSCE [5] has a form:

$$\beta_c(t) = \frac{t}{a + bt}. \tag{19}$$

Both approaches prove to give reliable results as long as the coefficients s as well as a and b are taken based on laboratory data for cements used in the concrete mix. The compressive strength development is then given as:

$$f_c(t) = \beta_c(t) f_{c,28}. \tag{20}$$

Tensile strength develops faster than compressive strength but not as fast as the modulus of elasticity. The standards follow the relationship between the compressive strength and the modulus of elasticity in which the time-development of the modulus is a square root of the time-development function used for determination of the compressive strength:

$$E_c(t) = k[f_c(t)]^{0.5}, \qquad (21)$$

where k is a material constant. Such an approach is also used for definition of the tensile strength, $f_t(t)$. Only the Eurocode 2 states that for early-age concrete ($t < 28$) the same time-development function can be used for both compressive and tensile strength development and that the exponent in Eq. 21 for the modulus of elasticity time development with respect to the compressive strength should equal to 0.3.

To account for the influence of elevated temperatures generated in concrete during hardening the equivalent age of concrete, t_e, can be used instead of real time. The equivalent age is determined based on the maturity method governing the Arrhenius law. The use of the equivalent age of concrete requires the knowledge of the temperature development profile during the analysed period.

The viscous effects in early-age concrete (creep) are accounted by introduction of the effective modulus of elasticity. The age-adjusted effective modulus method was proposed in which the effect of creep was accounted by reduction of the modulus of elasticity [14]:

$$E_{c,\text{eff}}(t) = \frac{E_c(t)}{1 + \rho(t, t_0)\varphi(t, t_0)}. \qquad (22)$$

The ageing coefficient varies within narrow range of 0.5 to 1.0 and can be assumed constant at $\rho(t,t_0)$ for many practical problems [14]. The creep coefficient is suggested to be taken as equal to 0.6 for early-age concrete [15].

3. RESTRAINT STRESSES IN X-RAY SHIELDING WALL

3.1. Cracking of an X-ray radiation shielding wall

The discussed wall is a structural element of an X-ray radiation shielding bunker. The structure is constructed to accommodate an X-ray machine to screen the trucks. The structure of the building consists of a steel shade roof with insulated sandwich panels supported by two reinforced concrete walls and foundations.

There are two main load-bearing reinforced concrete walls. The first RC wall (wall no. 1) is 0.5 m thick, reinforced with 2 layers of 16 mm steel bars in both directions. The total height of the wall is 6.4 m with a construction joint at 1.1 m from the bottom. The total length of the wall is 47.9 m. The second RC wall (wall no. 2) is 0.85 mm thick, also reinforced with 2 layers of 16 mm steel bars in both directions. The total
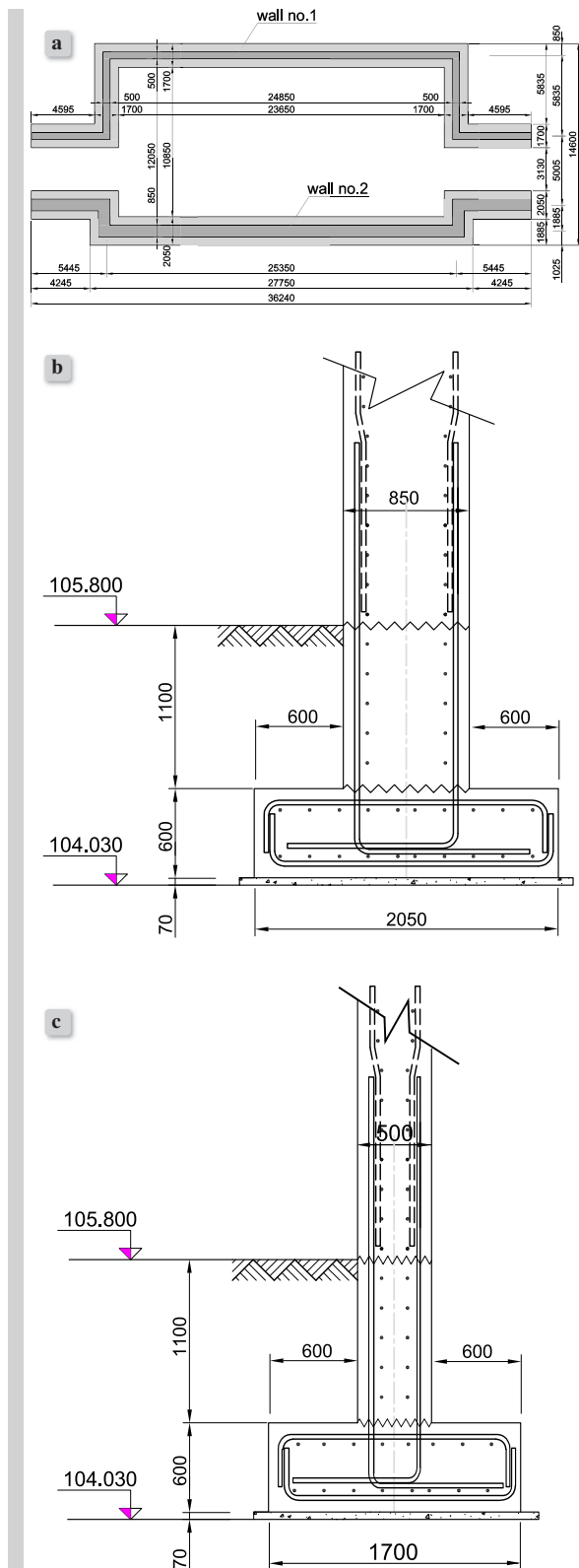
Figure 4.
Geometry of the X-ray shielding walls
a. top view, b. wall no. 1, c. wall no. 2

height of the wall is 6.3 m with a construction joint at 1.1 m from the bottom. The total length of the wall is 40.0 m. Geometry of the walls is presented in Fig. 4.

The walls were made of normal-weight concrete with design strength of 35 MPa (C35/45), however, the actual concrete strength ranged from 43 MPa to 55 MPa. According to the mix design, 400 kg of Type I cement was used with a water-to-cement ratio of 0.44. The detailed concrete mix composition is given in Table 1.

Table 1.
Composition of concrete mix used for X-ray shielding wall

component	content [kg/m³]
cement	400
water	175
coarse aggregate 5/10 mm	412
coarse aggregate 10/20 mm	814
fine aggregate 0/5 mm	665
admixture	3
Density	**2469**

Both walls were cast in two stages. Wall in stage one was cast from the top of foundation up to the ground level (1.1 m height), and in the stage two was cast from ground level up to 5.3 m from the ground. Wall no. 1 (0.5 m) was cast on 12th February 2014 (stage 1, 29 m³ of concrete) and on 18th March 2014 (stage 2, 128 m³). Wall no. 2 (0.85 m) was cast on 18th February 2014 (stage 1, 42 m³ of concrete) and on 9th April 2014 (stage 2, 177 m³).

According to the Köppen-Geiger climate classification the location of the construction site can be classified to the BWh climate (a hot, dry desert climate with the annual average temperature above 18°C). The detailed historical weather data for the location were taken from the weather information portal http://weatherspark.com. Diagrams in Fig. 5 present the temperature, humidity and wind velocity variations for the quarter of 2014 in question. Steady monotonic increase of temperature was observed over that period; the minimum average temperature was increasing from approx. 17 to 25°C while the maximum from approx. 27 to 34°C. The average diur-
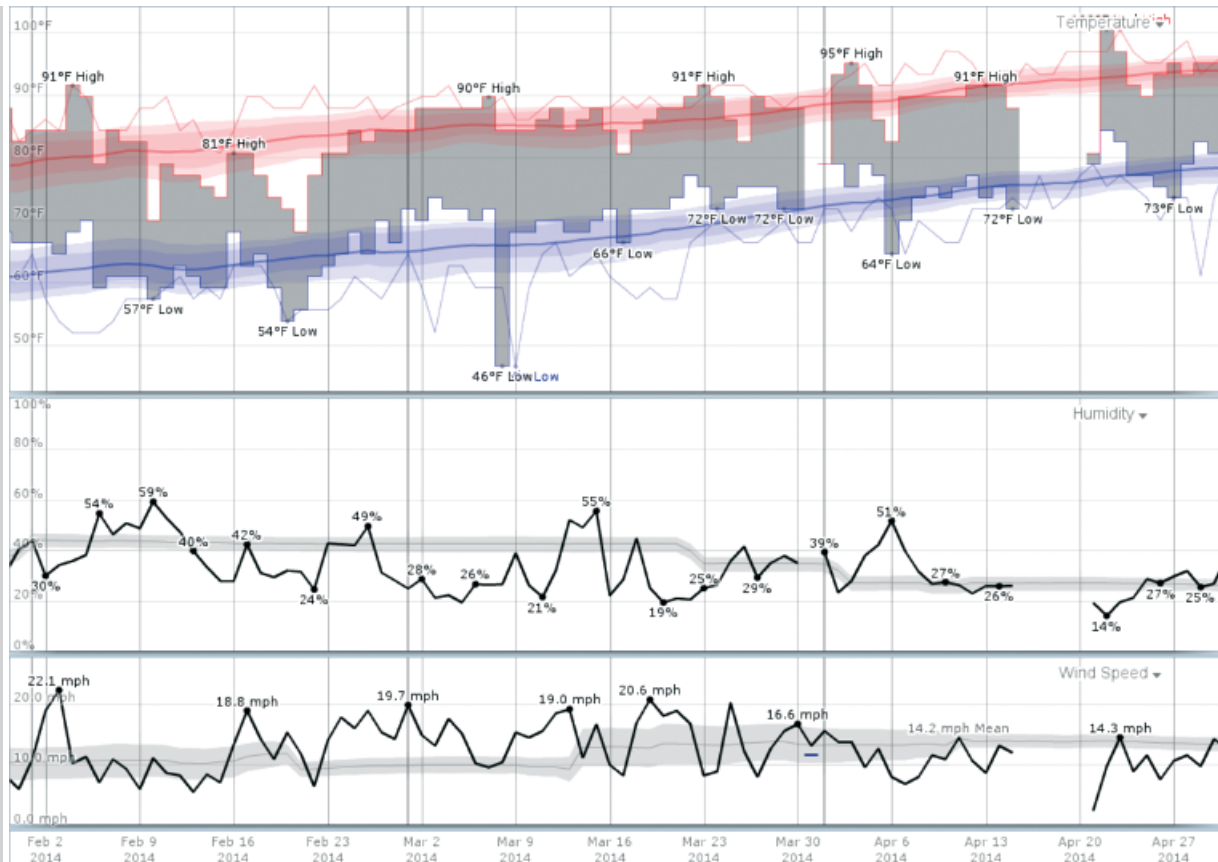
Figure 5.
Weather conditions during execution and curing of the structure (http://weatherspark.com)
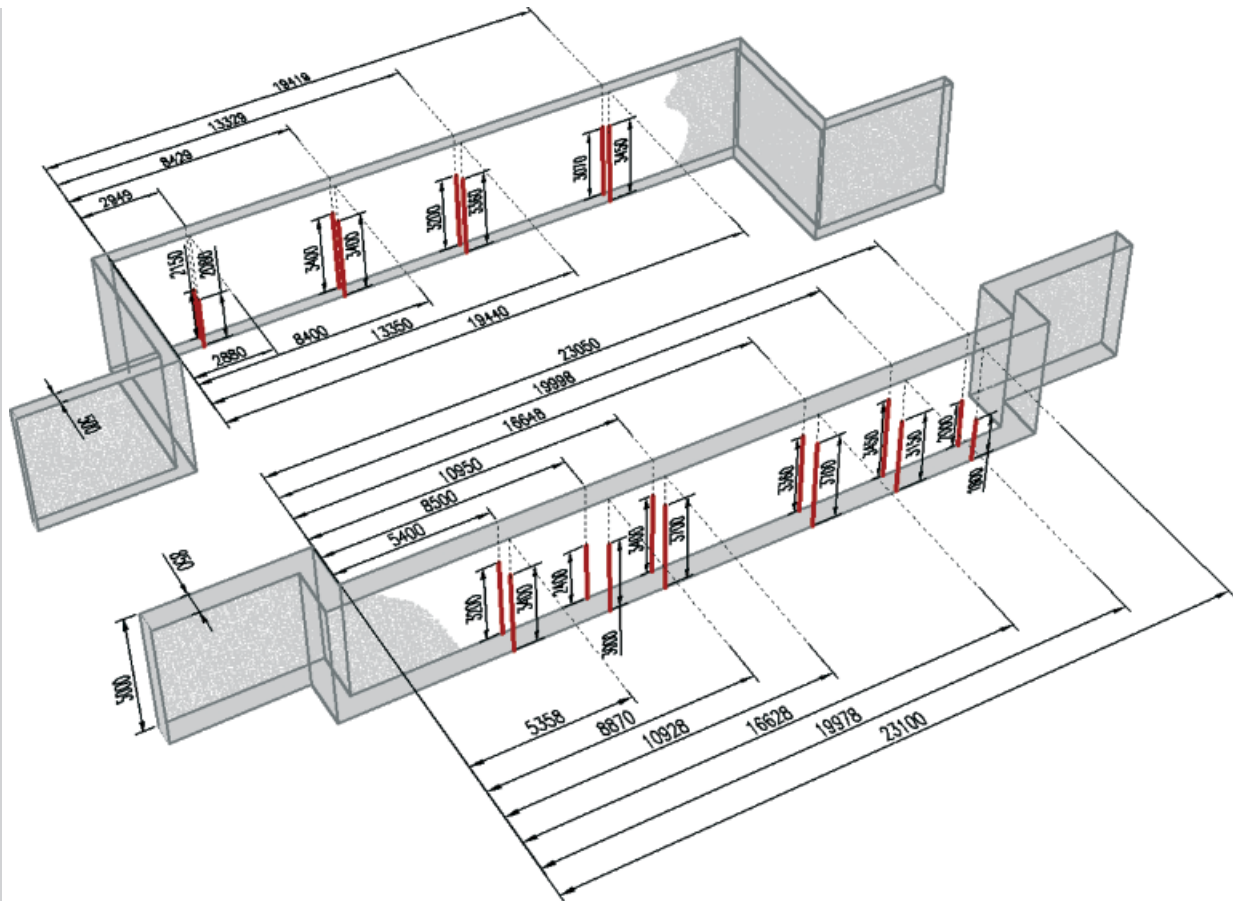
Figure 6.
Cracking pattern in load-bearing walls

nal change of temperature was equal to approx. 10°C. Relative humidity varied between 20% and 55% with mean value of 43% in February and first half of March, decreasing to 35% in the second half of March and 27% in April. Due to the coastal location of the construction site large wind speed variations were observed. In the first period, i.e. up to the middle of March mean wind velocity was equal to 4.7 m/s and in the second phase increased to 6.0 m/s. However, wind speed reached even up to 9.0 m/s.

After removing the formworks, the concrete wall was fully covered with a wet hessian for 7 days. When curing has completed, cracks were observed on each side of the wall: there were 4 cracks in the first wall and 6 cracks in the second wall. The cracks reached up to 3.5 m of the wall's height (Fig. 6). The cracks width ranged from 0.1 mm to 0.2 mm. Photos of a chosen crack are presented in Fig. 7. Location of the cracks suggests that the cracks might be through cracks.

3.2. Calculation of stresses in radiation shielding wall

Determination of the temperature time-development and distribution in early-age structure is an extremely difficult task. Unless exact laboratory material data as well as environmental and technological conditions are known, thermal analysis is just estimation. Calculation of temperature variations in the concrete element requires solution of the heat equation for which the material data such as thermal conductivity, λ, and specific heat of concrete, c_b, as well as hydration heat development of cement, $Q(t)$, must be known. For the solution of the heat equation third type boundary condition is used which defines the heat flow driven by the temperature difference between the structure and the ambient environment $(T_{sur} - T_a)$. The flow is proportional to that difference with the proportionality factor being the heat transfer coefficient, α_p, which value is strongly dependent on the wind speed. Thus, the weather conditions highly
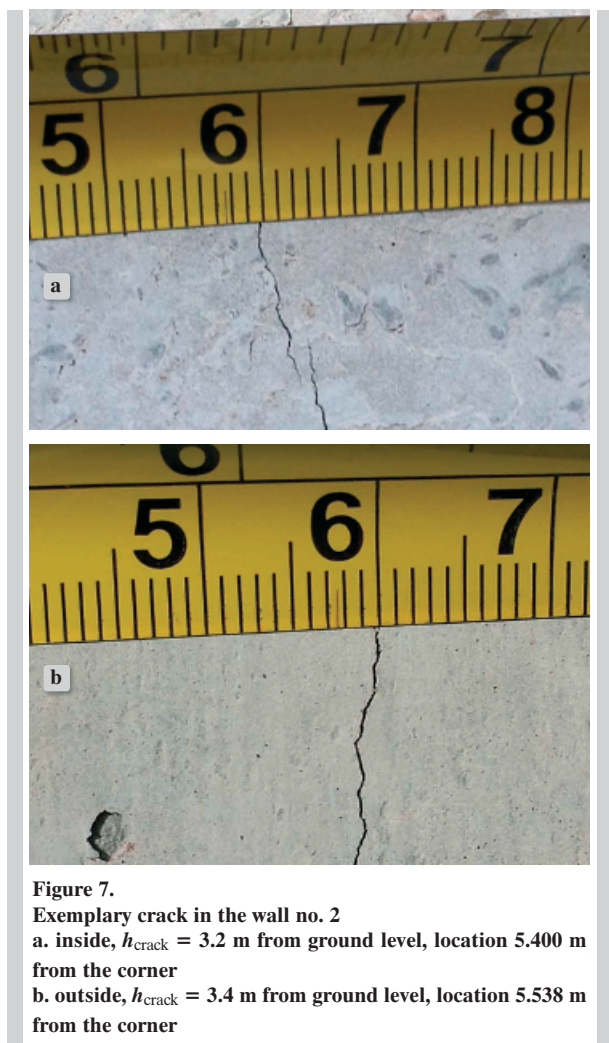
Figure 7.
Exemplary crack in the wall no. 2
a. inside, h_{crack} = 3.2 m from ground level, location 5.400 m from the corner
b. outside, h_{crack} = 3.4 m from ground level, location 5.538 m from the corner

influence the heat transfer in the structure-environment system and the temperatures generating in the element. Similar considerations can be made when analysing moisture variations. Given the limitations of the analysis the predicted temperature, temperature difference and shrinkage in the analysed elements was only estimated, however, this estimation should be discussed.

The massiveness of the walls was determined with a simple formula $m = 2/d$ assuming that in the elements with such a simple geometry the equivalent thickness is equal to half of the real thickness of the element. The walls are then characterised with the massiveness equal to 2.35 m^{-1} for the wall no. 1 and 4.00 m^{-1} for the wall no. 2. This means that both walls are medium-thick elements. The expected temperature increase according to recommendations of Flaga would be ~17°C and 19°C, respectively. However, these values are definitely underestimated. It was

shown by Klemczak and Knoppik-Wróbel [16, 17] that in the walls of thickness and concrete composition similar to those of the analysed walls, regardless of the initial temperature of concrete and ambient temperature during curing, the expected temperature increase in the interior of the walls would amount to ~30°C and 35°C, respectively. Given the geometry, the expected temperature difference between the interior and the surface of the wall would be equal to ~5°C and 8°C. Due to high wind speeds (much higher than in the referred analyses) the actual temperature gradients were most probably higher.

The calculations were performed for the wall no. 2. For determination of thermal strain the temperature difference during cooling needs to be known. The data about temperature development in walls was scarce. Assuming that the temperature of concrete mix was equal to the ambient temperature at the moment of execution, temperature in the wall no. 2 increased by 35°C and the wall cooled down to the temperature of the surrounding air, which over the period of execution of the walls increased by about 2°C, temperature difference during cooling was taken as ΔT_M = 33°C and the differential temperature accounting for heating of the restraining element as ΔT_M^* = 29.7°C. The strain difference due to internal stresses was determined for temperature difference of ΔT_S = 4°C. Assuming the value of thermal dilation coefficient α_T = 10^{-6}/°C the resulting thermal strain along compensation line was equal to ε_T^* = 2.97·10^{-4} and additional strain at the surface due to internal restraint was equal to $\Delta\varepsilon_T$ = 0.40·10^{-4}.

Given that the wall was wet-cured the influence of drying shrinkage was neglected. Autogenous shrinkage was assumed as uniform over the volume of the wall and was determined according to recommendations of Eurocode 2. After 7 days of curing the calculated shrinkage of the wall amounted to $\varepsilon_{ca}^{II}(t^{II})$ = 0.40·10^{-4} while over that period the shrinkage in the previous stage of the wall (stage 1 of the wall no. 2) increased by $\varepsilon_{ca}^{I}(t^I+t^{II})$ - $\varepsilon_{ca}^{I}(t^I)$ = 0.04·10^{-4}. The differential shrinkage strain was equal to ε_{ca}^* = 0.36·10^{-4}, which is equivalent to temperature change of $\Delta T_{M,eq}$ = 3.6°C.

The analysed walls are characterised with the length-to-height ratios of 9.0 and 7.7 for the wall no. 1 and wall no. 2, respectively. It should be noted that the L/H ratio of the walls is a rough estimation because of the complex shape of the walls. Nevertheless, the analysed walls are undoubtedly long walls. Moreover, the character of the cracks, which appeared only in a

central part of the wall and are all of almost the same height and vertical in direction, signifies that the restraint stresses which caused these cracks were exerted mainly due to the influence of the horizontal translational restraint. Hence, the restraint thermal stress was calculated as follows:

$$\sigma_{ext} = R\,\varepsilon_{tot}\,E_{c,eff}\ , \tag{23}$$

with:

$$\varepsilon_{tot} = \varepsilon_T^* + \varepsilon_{ca}^*\ , \tag{24}$$

$$R\!\left(R_N^0,\delta_{res}^0,h\right) = \delta_{res}^0(h)R_N^0\ , \tag{25}$$

and the additional self-induced stress:

$$\sigma_{int} = \Delta\varepsilon_T\,E_{c,eff}\ . \tag{26}$$

The crack was defined at the height were $\sigma_T(h) > f_t(t)$. Tensile strength $f_{ctm}(t)$ and modulus of elasticity $E_{cm}(t)$ were calculated with the approach given by Eurocode 2 [12]:

$$f_{cm} = f_{ck} + 8\text{MPa}\ \ \text{and}\ \ f_{cm}(t) = \beta_c\,f_{cm}\ , \tag{27}$$

$$f_{ctm} = 0.3\!\left(f_{cm}\right)^{2/3}\ \text{and}\ \ f_{ctm}(t) = \beta_c\,f_{cmt}\ , \tag{28}$$

$$E_{cm} = 22.1\!\left(0.1f_{cm}\right)^{0.3}\ \text{and}\ \ E_{cm}(t) = \beta_c^{0.3}\,E_{cm}\ , \tag{29}$$

with β_c acc. to Eq. 18. Their values were determined for $t = 7$ days. Given the characteristic value of the compressive strength $f_{ck} = 35$ MPa: $f_{ctm}(7) = 2.75$ MPa, $E_{cm}(7) = 32.5$ GPa and $E_{cm,eff} = 21.96$ GPa. $E_{cm,eff}$ was calculated according to Eq. 22. Analogically, for the hardened concrete of foundation the modulus of elasticity was also determined with this method. The fixation stress was calculated to be equal to $\sigma_{fix} = 7.31$ MPa while self-induced stress was calculated to be equal to $\sigma_{int} = 0.88$ MPa.

Restraint coefficient was calculated as a product of the plane-section translational coefficient and resilience factor (Eq. 18). The plane-section translational coefficient was calculated as follows [2, 4]:

$$R_N^0 = \frac{1}{1 + \dfrac{A_F E_F}{A_c E_c}}\ . \tag{30}$$

In the calculations the area of the restraining body (denoted with index F) was calculated assuming that both the foundation and stage 1 of the wall being mature exerted a restraint to the stage 2 of the wall. Stage 2 (denoted with index c) was taken as the early-age part of the wall (see Fig. 8). The value of the fac-

tor was equal to 0.339. The restraint stress due to translational restraint was calculated to be equal to $\sigma_{ext}^0 = 2.48$ MPa.

To determine the resilience factor, the diagrams can be used. However, because the use of diagrams is not convenient, the ACI Report 207 provided a formula to calculate distribution of resilience factor at the height of the wall. For long walls the formula has a form:

$$\delta_{res}^0(h) = \left(\frac{L/H - 2}{L/H + 1}\right)^{h/H}\ . \tag{31}$$
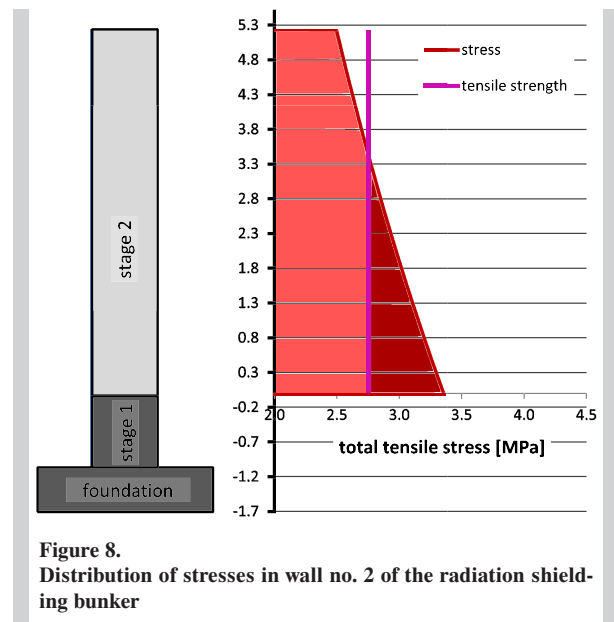
Figure 8.
Distribution of stresses in wall no. 2 of the radiation shielding bunker

The resulting resilience factor for the wall no. 2 varied from 1 at the joint to 0.655 at the top of the wall. Diagram in Fig. 8 presents distribution of stresses at the height of the wall considering the early-age (stage 2) concrete. Level 0 refers to the location of the old concrete–new concrete joint. The total tensile stress decreases from the maximum value of $\sigma_{ext} + \sigma_{int} = 3.36$ MPa according to the resilience factor to reach 65.5% of this value (2.50 MPa) at the top-most fibres. Taking into account the value of tensile strength, which was assumed as equal at the whole height, the calculated height of the crack reached $h_{crack} \approx 3.4$ m at the surface of the wall. It must be emphasised that in reality there is also temperature gradient at the height of the wall which determines the distribution of thermal stress; the value of tensile stress is smaller near the joint – its character is similar to what was presented in Fig. 5. Moreover, the rate of tensile strength development

depends on the temperature so due to different values of temperature tensile strength would also vary throughout the wall. Nevertheless, for analytic calculations such simplifications can be made.

4. DISCUSSION AND CONCLUSIONS

The presented simplified approach is very convenient from the practical point of view. As it was shown, the cracking risk of early-age walls depends on many factors, some of which can be controlled and some of which are very difficult to control or just unknown. The cracking risk in walls depends mostly on the temperature change during cooling, ΔT_M (which can be a sum of the actual temperature change and equivalent temperature change due to shrinkage), thermal gradient at the thickness of the wall, ΔT_S, and the degree of restraint which can be expressed with a restraint factor, R. Since the restraint factor depends mainly on geometrical characteristics of the element and is a known value, the design and – especially – execution and curing of the wall should concentrate on limitation of the temperature change in the following way [18]:

$$\Delta T_{\text{allow}} = \frac{\varepsilon_{tsc}}{K \alpha_T R},\qquad(32)$$

where:

ε_{tsc} – tensile strain capacity of concrete;

K – modification factor for sustained loading and creep;

α_T – coefficient of thermal expansion, 1/°C.

Given the ambient environmental conditions during execution and curing of the structure the temperature change can be limited most of all by appropriate design of concrete mix. It is also advised to pre-cool concrete mix before casting concrete at the construction site. The wall should not be exhibited to thermal shock by too early removal of insulation and/or formwork. In important massive concrete structures the temperature should be measured continuously during hardening of concrete and unexpected temperature changes should be instantaneously accommodated.

Nevertheless, it must be remembered that restraint stresses have major impact on the total thermal stresses in early-age walls. Thus, the degree of restraint should be minimised by decreasing the length of the element, the stiffness of the restraining body of the degree of the reinforcement at the joint.

ACKNOWLEDGEMENTS

REFERENCES

[1] *Klemczak B., Knoppik-Wróbel A.*; Analysis of early-age thermal and shrinkage stresses in reinforced concrete walls, ACI Structural Journal, 2014; Vol.111, No.2, p.313-322

[2] *Nilsson M.*; Restraint factors and partial coefficients for crack risk analyses of early age concrete structures, PhD thesis, Luleå University of Technology, Luleå 2003

[3] *Flaga K.*; Naprężenia skurczowe i zbrojenie przypowierzchniowe w konstrukcjach betonowych (Shrinkage stresses and surface reinforcement in concrete structures), Monograph 391, 2$^{\text{nd}}$ edition, Wydawnictwo Politechniki Krakowskiej, Kraków 2011 (in Polish)

[4] ACI Committee 207; Report on thermal and volume change effects on cracking of mass concrete (ACI 207.2R-07), ACI Manual of Concrete Practice, Part 1, 2007

[5] Japan Society of Civil Engineers; JSCE Guidelines for concrete. No. 15: Standard Specifications for concrete structures. Design, 2011

[6] PN-EN 1992-3. Eurocode 2 – Design of concrete structures – Part 3: Liquid retaining and containment structures, 2008

[7] *de Schutter G., Taerwe L.*; Early-age thermal cracking tendency of massive concrete elements by means of equivalent thickness, ACI Materials Journal, 1996; Vol.93, No.5, p.403-408

[8] *Klemczak B., Knoppik-Wróbel A.*; Comparison of analytical methods for estimation of early-age thermal-shrinkage stresses in RC walls, Archives of Civil Engineering, 2013; Vol.59, No.1, p.97-117

[9] *Emborg M.*; Thermal stresses in concrete structures at early ages, PhD thesis, Luleå University of Technology, Luleå 1989

[10] PN-EN 1992-3. Eurocode 2 – Design of concrete structures – Part 1-1: General rules and rules for buildings, 2008

[11] *Flaga K.*; Naprężenia własne termiczne typu "makro" w elementach i konstrukcjach z betonu ("Macro" type self-induced thermal stresses in concrete elements and structures), Monograph 106, Wydawnictwo Politechniki Krakowskiej, Kraków 1990 (in Polish)

[12] CEP-FIP; *fib* Model Code for Concrete Structures 2010, Ernst & Sohn, 2013

[13] ACI Committee 209; Report on prediction of creep, shrinkage and temperature effects in concrete structures (ACI 209R-92), ACI Manual of Concrete Practice, Part 1, 1997

[14] CEP-FIP; fib Bulletin 70. State-of-the-art report: Code-type models for concrete behaviour. Background of MC2010, 2013

[15] *Kiernożycki W.*; Betonowe konstrukcje masywne (Massive concrete structures), Polski Cement, Kraków 2003 (in Polish)

[16] *Klemczak B., Knoppik-Wróbel A.*; Early-age thermal and shrinkage cracks in concrete structures – influence of geometry and dimensions of a structure, Architecture – Civil Engineering – Environment, 2011; Vol.4, No.3, p.55-70

[17] *Klemczak B., Knoppik-Wróbel A.*; Early-age thermal and shrinkage cracks in concrete structures – influence of curing conditions, Architecture – Civil Engineering – Environment, 2011; Vol.4, No.4, p.47-58

[18] *Bamforth P. B., Price W. F.*; Concreting deep lifts and large volume pours, Construction Industry Research and Information Association, London 1995